

Supplementary information

Selective hydrogenation of 5-hydroxymethylfurfural and its acetal with 1,3-propanediol to 2,5-bis(hydroxymethyl)furan using supported rhenium-promoted nickel catalysts in water

Jan J. Wiesfeld^a, Minjune Kim^b, Kiyotaka Nakajima^{b,c*}, Emiel J.M Hensen^{a*}

^a Laboratory of Inorganic Materials and Catalysis, Schuit Institute of Catalysis, P.O. Box 513, 5600 MB Eindhoven, Eindhoven University of Technology, The Netherlands

^b Institute for Catalysis, Hokkaido University, Kita 21 Nishi 10, Kita-ku, Sapporo 0010021, Japan

^c Advanced Low Carbon Technology Research and Development Program (ALCA), Japan Science and Technology Agency (JST), 4-1-8 Honcho, Kawaguchi 332-0012, Japan.

* To whom correspondence should be addressed, e.j.m.hensen@tue.nl,
nakajima@cat.hokudai.ac.jp

Contents

- 1. Literature survey of catalytic hydrogenation of 5-HMF**
- 2. Characterization of prepared catalysts**
- 3. Supplementary catalytic data**
- 4. References**

Table S1. Literature survey of catalytic hydrogenation of 5-HMF to BHMF and BHMTHF

#	Catalyst	HMF conc. (mol L ⁻¹)	Solvent	<i>V</i> (mL)	<i>P</i> _{H2} (MPa)	<i>T</i> (°C)	<i>t</i> (h)	Conv. (%)	Yield ^a (%)	Ref.
1	Ni/SiO ₂ (10 wt% Ni, 100 mg)	0.5	H ₂ O ^b	10	8.0	40	0.5	~5	~ 5 (-)	1
2	Ni-Pd/SiO ₂ (Ni/Pd = 7, 2 wt% Pd, 100 mg)	0.5	H ₂ O ^b	10	8.0	40	2	99	<1 (96)	1
3	Pd/C (10 wt% Pd, 500 mg)	0.2	Dioxane	20	0.1	60	12.3	90	80 (-)	2
4	Pd-Ir/SiO ₂ (Ir/Pd = 1, 2 wt% Pd, 150 mg)	0.6	H ₂ O	9	8.0	2	1	99	- (95)	3
5	Pt/MCM-41 (1 wt% Pt, 100 mg)	2	H ₂ O	2	0.8	35	2	100	98.9 (-)	4
6	Cu/SiO ₂ (56 wt% Cu, 500 mg)	1.6	MeOH	50	2.5	100	8	100	97 (-)	5
7	Ir-ReOx/SiO ₂ (Ir/Re = 1, 4 wt% Ir, 50 mg)	1	H ₂ O	3	0.8	30	6	> 99	> 99 (-)	6
8	NiRe _{0.5} /TiO ₂ (Re/Ni = 0.5, 3 wt% Ni, 10 mg)	0.5 ^c	H ₂ O ^d	2	5.0	40	4	99	89 (3)	This work

[a] Represents yields of BHMF and BHMTHF (in parentheses).

[b] 0.02 equivalents of acetic acid used as additive.

[c] PDHMF was used as substrate instead of HMF.

[d] 0.001 equivalents of Na₂CO₃ used as additive.

2. Characterization of prepared catalysts

Table S2 lists the most important properties of the catalysts. For comparing purposes, monometallic Ni/TiO₂ and Re/TiO₂ were also included in this study. We found that actual rhenium weight loadings are systematically 15% higher than those desired and we expect this is due to the nature of the aqueous rhenium precursor solution used.

Table S2. Catalyst notation and metal loadings.

Catalyst	Ni loading ^[a] (wt%)	Re loading ^[a] (wt%)	Re / Ni (mol / mol)
Ni	2.97	-	-
NiRe _{0.5}	2.92	5.50	0.593
NiRe ₁	2.91	10.8	1.17
NiRe ₂	2.82	20.5	2.29
Re	-	11.3	-

[a] Determined by ICP-OES.

XPS was used to determine the surface composition of the catalysts to further elucidate the nature of the active site and the trend found with chemisorption. Deconvoluted spectra are provided in Figure S1 and quantitative surface contributions are summarized in Table S3. Low levels of rhenium (NiRe_{0.5}) significantly enhance the nickel dispersion due to the largest value of Ni/(Ni+Ti) in Table S3. Further increase of rhenium content (NiRe₁ and NiRe₂) lowers the overall nickel dispersion; however, the surface concentration of metallic nickel remains relatively stable at the expense of oxidized nickel. We also observe a large heterogeneity of Re species ranging from metallic rhenium, Re²⁺, Re⁴⁺, Re⁵⁺, Re⁶⁺ and Re⁷⁺. Increasing the rhenium loading increases the amount of metallic rhenium after reduction at the expense of the oxidized species. Re/TiO₂ has a rhenium species distribution comparable to NiRe_{0.5}/TiO₂. Kaituo *et al.* showed that nickel and rhenium are distributed as bimetallic particles.⁷ It is possible that rhenium prefers to reside on the outside of the particle. If we then assume that metallic nickel makes up the bulk of the active sites, it is likely that a portion of the active sites are covered with rhenium, which would explain the trend observed by chemisorption (Table S4).

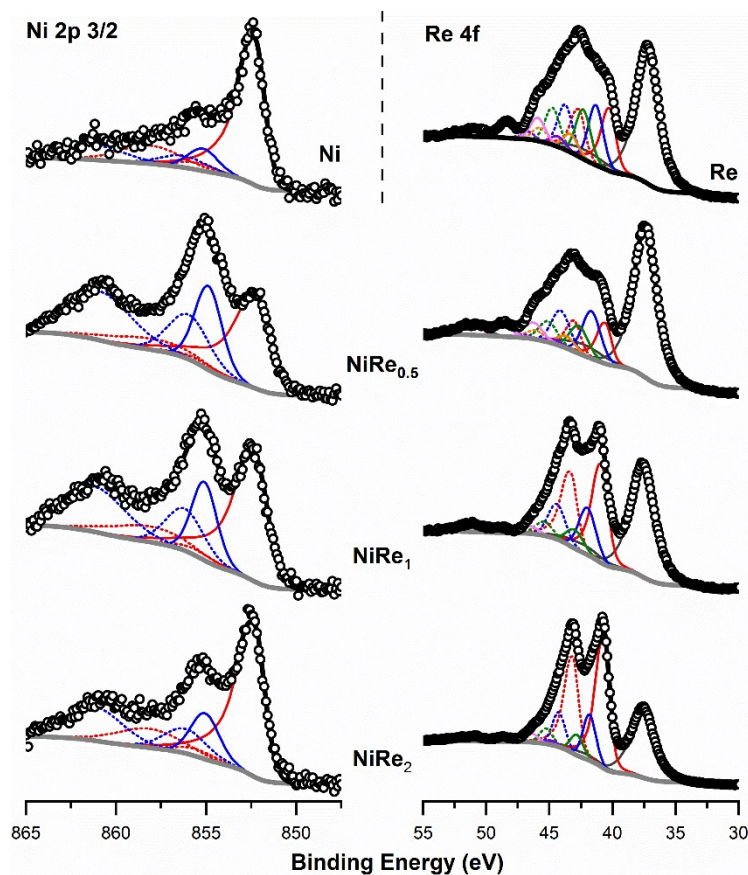


Figure S1. Ni 2p^{3/2} and Re 4f XPS spectra of titania-supported Ni, Re and bimetallic catalysts. Experimental data is represented by open circles and the fit by a black curve. The Ni 2p^{3/2} fits (left) are composed of Ni⁰ (red) and Ni²⁺ (blue) and corresponding satellite signals (dotted lines). Re 4f fits comprise Re⁰ (red), Re²⁺ (blue), Re⁴⁺ (green), Re⁵⁺ (orange), Re⁶⁺ (violet), Re⁷⁺ (pink), as well as signals belonging to Ti 3p (gray).

Table S3. Summary of quantified XPS data for TiO₂-supported Ni, Re and NiRe_x catalysts.

Catalyst	Ni ⁰ (at%)	Ni ²⁺ (at%)	Re ⁰ (at%)	Re ^{x+} [a] (at%)	Ti (at%)	Ni/(Ni+Ti) (at%)	Re/(Re+Ti) (at%)	Ni/Re -
Ni	0.76	0.27	-	-	26.77	3.71	-	-
NiRe _{0.5}	1.37	1.89	0.58	1.64	23.64	12.11	8.58	1.47
NiRe ₁	1.20	1.17	1.78	1.19	23.45	9.18	11.24	0.80
NiRe ₂	1.14	0.71	4.23	2.06	23.27	7.36	21.25	0.29
Re	-	-	1.05	2.34	23.98	-	12.39	-

[a] Sum of all oxidic rhenium species.

Figure S2 summarizes the result of the H₂-TPR characterization of the catalysts. We observe that reduction of nickel on Ni/TiO₂ takes place around a temperature 300 °C, which increases upon increasing amounts of rhenium. Reduction of rhenium on Re/TiO₂ starts at roughly 310 °C and only reaches a maximum at 350 °C. We can also appreciate that the total hydrogen uptake (Table S4) is significantly larger for the bimetallic catalysts than for the monometallic materials. Ni has a H₂/metal ratio of 1.23, which increases linearly with the amount of rhenium for NiRe_{0.5} and NiRe₁ but reaches a plateau for NiRe₂. Re itself has a H₂/metal ratio of 2.9, significantly higher than that of Ni, which is attributed to the higher maximum oxidation state of Re vs. Ni (+7 vs. +2). This makes any attempt to calculate the degree of reduction quite challenging based on TPR results alone. However, the XPS data (Table S3) shows that ~75% of the nickel is fully reduced on Ni/TiO₂. In NiRe_{0.5}, the relative amount of reduced Ni dropped to ~40%, but the absolute surface abundance is nearly doubled. Interestingly, the absolute amount of Ni⁰ stays roughly the same with increasing amounts of rhenium, although the total nickel surface abundance drops. This implies that higher levels of rhenium increase the reducibility of Ni, which is contra-intuitive when judging the TPR profiles. Rhenium displays similar trends with respect to relative abundances of Re⁰ with increasing amounts of rhenium.

Table S4. Quantitative TPR results TiO₂-supported Ni, Re and NiRe_x catalysts.

Catalyst	H ₂ uptake ^[a] (mmol g ⁻¹)	H ₂ /M _{tot} ^[b] (mmol mmol ⁻¹)	[Active sites] ^[c] (mmol g ⁻¹)	d _{av} ^[d] (nm)	D ^[d] (%)
Ni	0.62	1.23	0.139	2.67	27.6
NiRe _{0.5}	1.37	1.72	0.602	1.60	75.9
NiRe ₁	2.29	2.23	0.583	2.34	54.2
NiRe ₂	3.75	2.37	0.404	5.10	25.6
Re	1.78	2.93	0.257	3.21	42.4

[a] Determined by TPR.

[b] Measured by TPR based on total metal content.

[c] Calculated from extrapolation of the linear part of the chemisorption isotherm to the ordinate.

[d] Average diameter *d* and dispersion *D* estimated from chemisorption using total metal content.

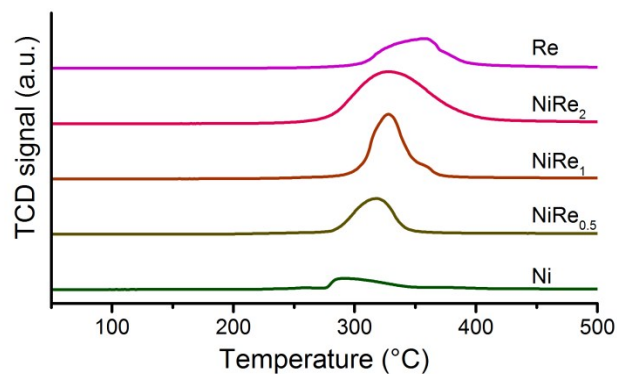


Figure S2. H₂-TPR profiles of TiO₂-supported Ni, Re, and NiRe_x catalysts.

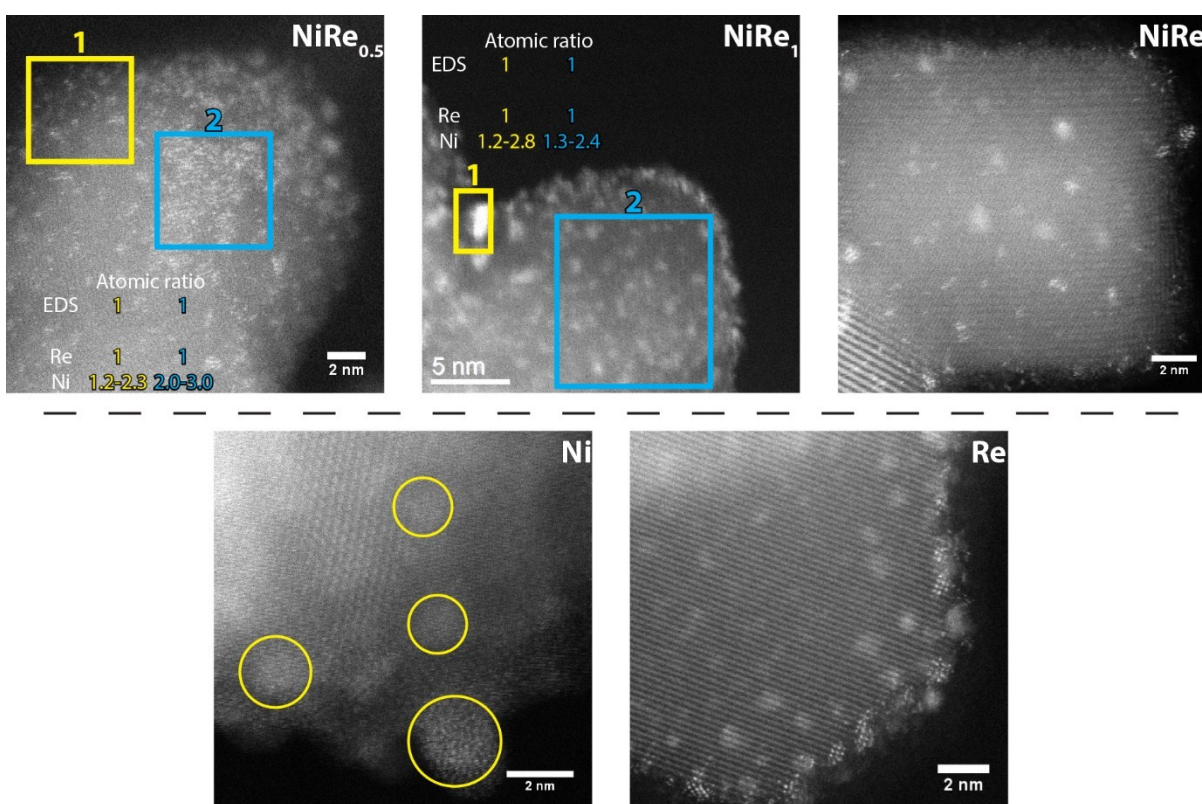


Figure S3. HAADF-STEM images for fresh Ni, Re and NiRe_x catalysts as well as EDS data for NiRe_{0.5} and NiRe₁. Ni particles on Ni/TiO₂ are highlighted with yellow circles as the contrast difference between nickel particles and the titania support is very low.

Figure S3 displays HAADF-STEM images for fresh Ni, Re and NiRe_x catalysts as well as EDS data for NiRe_{0.5} and NiRe₁. EDS data for NiRe₂ could not be generated due to technical difficulties. The particle size of Ni matches the one estimated from CO chemisorption (2.3 nm vs. 2.67 nm)

and this also holds for NiRe_{0.5} and NiRe₁. Average particle sizes of NiRe₂ and Re displayed by the HAADF-STEM images clearly differ from those measured by CO chemisorption. This indicates that only a fraction of the rhenium species can chemisorb CO, which results in overestimation of the particle size. The EDS data generated for NiRe_{0.5} and NiRe₁ confirms the close proximity or even bimetallic nature of the metal particles.

3. Supplementary catalytic data

Table S5. PDO degradation study in contact with NiRe₂ under reaction conditions. ^[a]

Substrate	X_{PDO} (%)	Y_{Unknown} (%)	C.B. ^[b] (%)
-	0.6	0.6	99.4
5-HMF	35.1	35.1	64.9
BHMF	3.6	3.6	96.4

[a] Reagents and conditions: NiRe₂ (10 mg), 1,3-PDO (1.1 mmol \pm 200 mg PDHMF), Substrate (200 mg), H₂O (2 mL), 1-butanol (1 μ L), H₂ (5 MPa), 40 °C, 750 rpm.

[b] Carbon balance.

Table S6. pH influence on the conversion and product distribution of 10% PDHMF, using NiRe_{0.5} as catalyst. ^[a]

Na ₂ CO ₃ eq / pH	X_{PDHMF} (%)	$Y_{5\text{-HMF}}$ (%)	Y_{BHMF} (%)	Y_{BHMTHF} (%)	Y_{PDHMTHF} ^[b] (%)	C.B. ^[c] (%)	PDO Rec. ^[d] (%)
5×10^{-1} / 11.4	52.1	0	1.0	2.2	40.8	91.9	84.5
1×10^{-1} / 11.2	52.7	0	1.2	2.4	39.8	90.6	82.5
5×10^{-2} / 11.1	53.4	0.2	1.0	2.4	42.0	92.0	86.2
1×10^{-2} / 10.9	53.1	1.7	22.4	1.5	20.0	92.2	91.7
5×10^{-3} / 10.7	50.8	0.7	31.4	2.2	15.6	99.9	96.0
1×10^{-3} / 10.4	99.2	1.2	89.0	3.4	0.8	95.1	93.0
1×10^{-3} / 10.4	98.9 ^[e]	56.0	34.1	< 0.1	< 0.1	91.2	95.7
5×10^{-4} / 10.2	98.8	2.1	86.0	6.9	0.3	96.5	94.5
0 / 7	94.4	8.5	78.7	5.0	< 0.1	92.5	91.8

[a] Reagents and conditions: Catalyst (10 mg), PDHMF (200 mg, molar ratio PDHMF/Ni = 214), H₂O (2 mL), 1-butanol (1 μ L), H₂ (5 MPa), 40 °C, 4 hours, 750 rpm

[b] 1,3-propanediol acetal of 5-hydroxymethyltetrahydrofurfural

[c] Carbon balance

[d] PDO recovery presented as a sum of unreacted PDHMF and free 1,3-propanediol. PDO originates from deprotection of PDHMF during the course of the reaction. It is excluded from the carbon balance.

[e] Conditions as [a] but using Ni as catalyst.

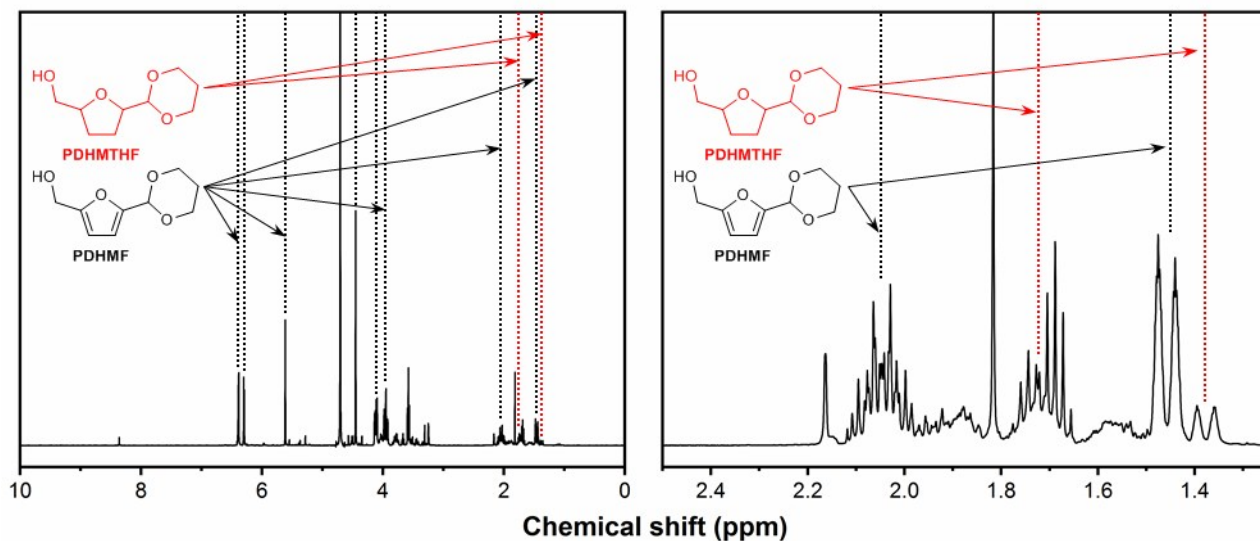


Figure S4. ^1H NMR spectrum of the reaction solution during PDHMF hydrogenation after 4 hours. Characteristic resonance signals for PDHMF (black) and PDHMTFH (red) are indicated with dotted lines. Reagents and conditions: PDHMF (200 mg), $\text{NiRe}_{0.5}$ (10 mg), Na_2CO_3 (0.5 eq. to PDHMF), D_2O (2 mL), 40°C , 4 h, H_2 (5.0 MPa).

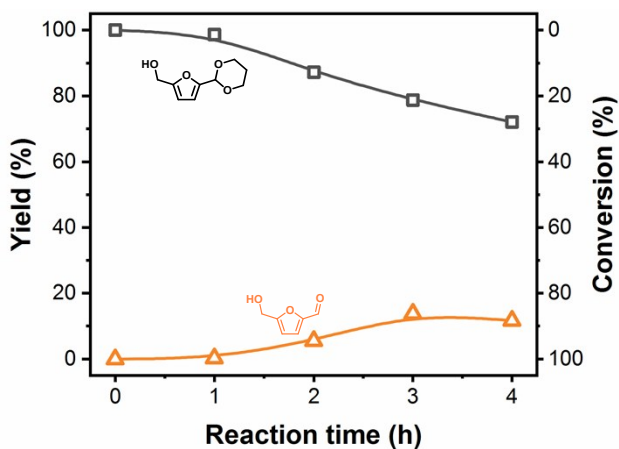


Figure S5. Time courses of PDHMF deprotection with $\text{NiRe}_{0.5}$. H_2 is replaced with N_2 . Lines provide guidance for the reader's eye. Reagents and conditions: Catalyst (10 mg), PDHMF (200 mg, molar ratio PDHMF/Ni = 214), H_2O (2 mL), 1-butanol (1 μL), N_2 (5 MPa), 40°C , 1×10^{-3} equivalence of Na_2CO_3 to PDHMF, 750 rpm.

4. References

- 1 Y. Nakagawa and K. Tomishige, *Catal. Commun.*, 2010, **12**, 154–156.
- 2 G. C. A. Luijkx, N. P. M. Huck, F. Van Rantwijk, L. Maat and H. Van Bekkum, *Heterocycles*, 2009, **77**, 1037–1044.
- 3 Y. Nakagawa, K. Takada, M. Tamura and K. Tomishige, *ACS Catal.*, 2014, **4**, 2718–2726.
- 4 M. Chatterjee, T. Ishizaka and H. Kawanami, *Green Chem.*, 2014, **16**, 4734–4739.
- 5 Q. Cao, W. Liang, J. Guan, L. Wang, Q. Qu, X. Zhang, X. Wang and X. Mu, *Appl. Catal. A Gen.*, 2014, **481**, 49–53.
- 6 M. Tamura, K. Tokonami, Y. Nakagawa and K. Tomishige, *Chem. Commun.*, 2013, **49**, 7034–7036.
- 7 K. Liu, J. Pritchard, L. Lu, R. Van Putten, M. W. G. M. Verhoeven, M. Schmitkamp, X. Huang, L. Lefort, C. J. Kiely, E. J. M. Hensen and E. A. Pidko, *Chem. Commun.*, 2017, **53**, 9761–9764.